INFORMATION CIRCULAR 49

PETROGRAPHIC ANALYSIS AND LITHIUM ISOTOPE GEOCHEMISTRY OF THE LOWER MEMBER OF THE SMACKOVER FORMATION IN THE BETSY SESSIONS NO. 1 WELL, UNION COUNTY, ARKANSAS

Stephen G. Franks and Peng Li

OFFICE OF THE STATE GEOLOGIST

Scott Ausbrooks, Director and State Geologist
North Little Rock, Arkansas

2026

STATE OF ARKANSAS

Sarah Huckabee Sanders, Governor

DEPARTMENT OF ENERGY AND ENVIRONMENT

Shane E. Khoury, Secretary

DIVISION OF ENERGY AND MINERAL RESOURCES

Alan York, Chief Administrator

OFFICE OF THE STATE GEOLOGIST

Scott Ausbrooks, Director and State Geologist



OFFICE OF THE
STATE GEOLOGIST

Table of Contents

DISCLAIMER 1
INTRODUCTION 1
PETROGRAPHIC ANALYSIS 2
LITHIUM ISOTOPIC ANALYSIS 11
CONCLUSIONS 15
REFERENCES 15

List of Figures

Figure 1. Jurassic stratigraphic column of southern Arkansas. 2

Figure 2. Composite photograph of a carbonate mudstone thin section from a depth of 7,379.90 ft, illustrating alternating organic-rich and organic-poor intervals. Superimposed letters (A–I) correspond to the specific locations of the high-resolution photomicrographs. Microfabric features include finely laminated organic-rich fabrics (A), homogenous organic-poor matrices (B–E, G), transitional features (F, H), and a distinct vertical fracture (I). All photomicrographs are captured under plane-polarized light unless otherwise specified (I, cross-nicols). 3

Figure 3. Plane-polarized light photomicrograph of organic-rich lamina at 7,379.90 ft. Fabric contains wavy organic strands (black), dispersed silt-sized quartz grains (bright white), and discontinuous, lensoidal micro-laminae of clear micrite embedded in a dark matrix. Scale bar is 0.5 mm. 4

Figure 4. High-magnification photomicrograph (plane light) at 7,379.90 ft showing a discontinuous, clear micrite micro-lamina (A) nested within dark, organic-rich micrite laminae (B). Scale bar is 100 µm. 4

Figure 5. Plane light photomicrograph of organic-poor laminae showing faint "ghosts" of rounded grains (0.3–0.5 mm). Yellow arrow denotes a prominent cloudy grain. Note the conspicuous absence of detrital quartz relative to Figure 2. Scale bar is 0.5 mm. 5

Figure 6. Composite photomicrographs (plane light) at 7,379.90 ft showing unidentified microfossils within the micrite matrix, including multi-locular chambered tests and ovate bioclasts. Scale bars are 100 µm. 5

Figure 7. Photomicrographs of a clear carbonate-filled microfracture within organic-poor micrite under plane light (left) and cross-polarized light (right). The fracture terminates at the

organic-rich laminae boundaries and displays a drusy fabric with crystal sizes increasing toward the center. Scale bar is 1 mm. 6

Figure 8. Thin section overview and photomicrographs of a poorly sorted peloidal packstone at 7,418.05 ft. Upper right: close-up of a large peloid. Lower right: representative grain size and poor sorting of the peloidal matrix. Lower left: bryozoan skeletal fragments and associated porosity (blue epoxy). All scale bars are 0.5 mm. 7

Figure 9. Photomicrograph (plane light) at 7,418.05 ft displaying a distinctive Favreina fecal pellet (center) characterized by internal, parallel longitudinal tubes. The pellet is surrounded by a poorly sorted peloidal packstone matrix. Scale bar is 0.5 mm..... 8

Figure 10. Thin section scan and plane-light photomicrographs at 7,441.90 ft. Lower panels: coarse, rhombohedral dolomitic siltstone with abundant organic matter (left) and a distinct, sharp-walled micrite layer with organic inclusions (right). Upper panels: finely interlaminated micrite and organic-rich siltstone highlighting low-angle downlapping geometries. All scale bars are 0.5 mm. 10

Figure 11. Comparison of the calculated Lower member of the Smackover organic matter δ^7Li composition (yellow star) against a global compilation of organic lithium isotope signatures from coals and petroleum source rocks (modified from Teichert et al., 2020). 14

List of Tables

Table 1. Whole rock X-ray diffraction (XRD) mineralogical data for the Lower member of the Smackover Formation core sample intervals (modified from Li et al., 2016) 11

Table 2. Geochemical data and lithium isotope compositions of core subsamples at 7,441.90 ft.12

Table 3. Calculated lithium concentrations and isotopic compositions (δ^7Li) for organic and inorganic phases within the 7,441.90 ft sample interval. 14

Petrographic Analysis and Lithium Isotope Geochemistry of the Lower Member of the Smackover Formation in the Betsy Sessions No. 1 Well, Union County, Arkansas

Stephen G. Franks and Peng Li

DISCLAIMER

This technical report was prepared under a collaborative agreement between RockFluid Systems, Inc. and the Arkansas Office of the State Geologist (AOSG). AOSG provided sample materials from its core repository, and RockFluid Systems, Inc. funded the associated laboratory analyses. As a public state agency, AOSG maintains a neutral stance and does not grant exclusive preference or endorsement to any specific client or collaborative research partner.

This document is published for general public information purposes. The authors make no warranty, express or implied, regarding the absolute accuracy, completeness, or suitability of the technical data provided by third parties. Any reliance the reader places on such information is strictly at their own risk, and the authors accept no liability for damages or losses resulting from the public use or misapplication of this report.

INTRODUCTION

Three core samples of the Lower member of the Smackover Formation (locally known as the Brown Dense) were collected from the Betsy Sessions No. 1 well in Union County, Arkansas (Fig. 1). These samples, obtained from the Norman F. Williams Sample Library, were previously analyzed by Li et al. (2016) to evaluate the source rock potential and physical properties of the Smackover Formation. This study extends that work by integrating detailed petrographic observations with lithium isotope geochemistry to investigate the lithium distribution between organic and inorganic components of the rock and estimate the lithium isotopic composition of the organic matter.

Thin sections from three core intervals were examined to characterize depositional fabrics, mineralogy, and diagenetic features. This petrographic analysis identified the 7,441.90 ft interval as ideal for lithium isotope testing due to its distinct, physically separable interlaminated organic-rich and organic-poor microfacies. Two isolated subsamples from these contrasting laminae were sent to Dr. Aaron Satowski at the University of Texas for lithium concentration and isotope

measurements. Aliquots of the same subsamples were analyzed for total organic carbon (TOC) by GeoMark Research, Ltd. in Houston, Texas.

The combination of petrographic observations, lithium concentrations, lithium isotope analyses, and TOC measurements provides the basis for a two-component mass-balance model. This model isolates and estimates the lithium concentration and isotopic composition of the organic matter from the surrounding inorganic matrix. Additionally, the petrographic observations provide geological context for interpreting these geochemical results.

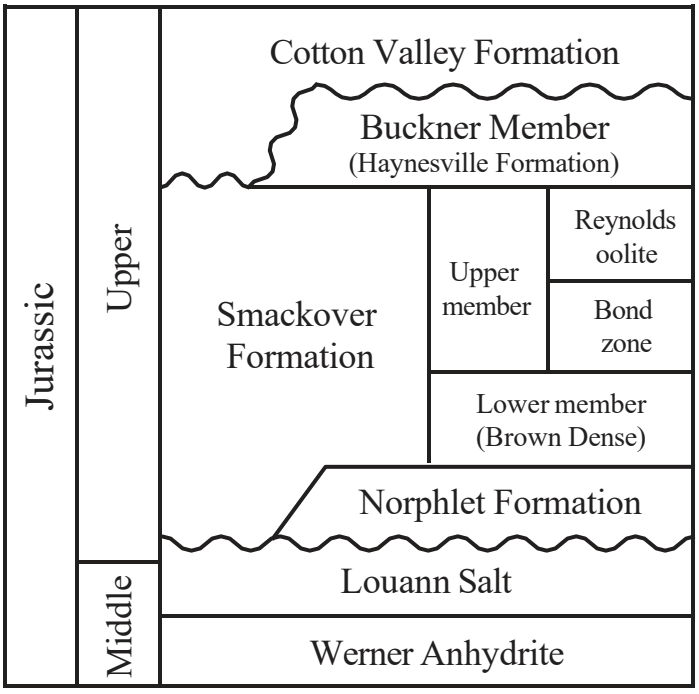

Figure 1. Jurassic stratigraphic column of southern Arkansas.

PETROGRAPHIC ANALYSIS

7,379.90 feet Interval (Micritic Mudstone)

The sample at 7,379.90 ft consists of alternating 3–5 mm thick organic-rich and organic-poor carbonate mudstone laminae (Fig. 2). The two microfacies are sharply defined, differing markedly in organic content, detrital grain abundance, and microfabric.

The dark organic-rich laminae contain abundant organic matter preserved as thin, wavy strands 1–10 μm thick (Fig. 3). These intervals also contain randomly dispersed, poorly sorted silt-sized quartz grains averaging approximately 0.04 mm in diameter. The quartz occurs throughout the organic-rich matrix rather than in discrete laminae. Within some organic-rich intervals, thin (<0.5 mm), discontinuous light-colored micrite laminae occur as lensoidal bodies enclosed by the darker organic-rich sediment (Figs. 3, 4).

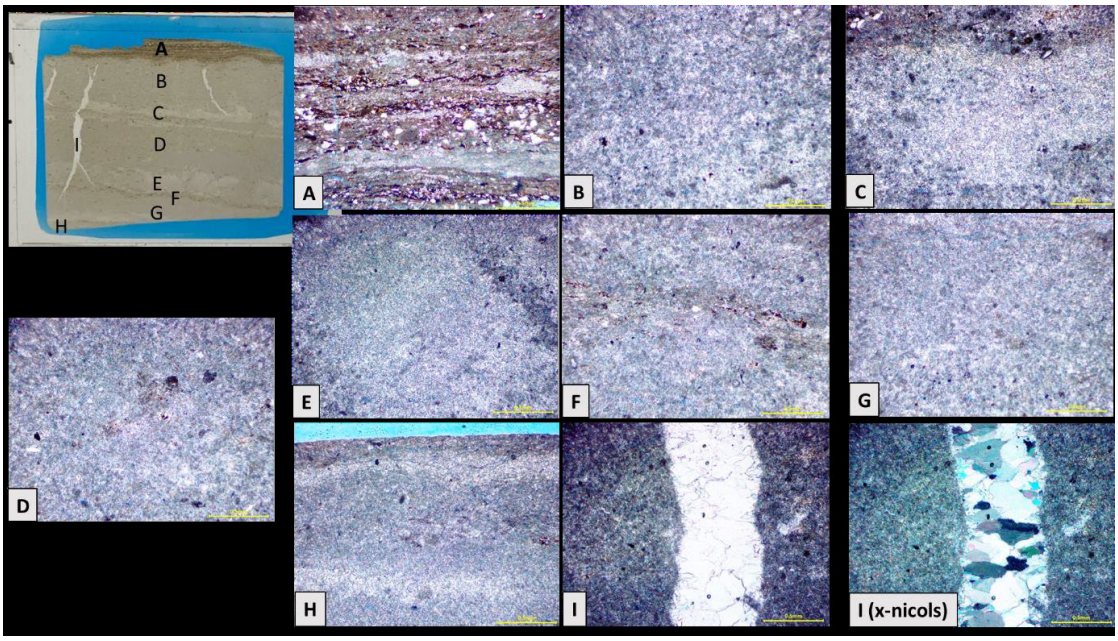

Figure 2. Composite photograph of a carbonate mudstone thin section from a depth of 7,379.90 ft, illustrating alternating organic-rich and organic-poor intervals. Superimposed letters (A–I) correspond to the specific locations of the high-resolution photomicrographs. Microfabric features include finely laminated organic-rich fabrics (A), homogenous organic-poor matrices (B–E, G), transitional features (F, H), and a distinct vertical fracture (I). All photomicrographs are captured under plane-polarized light unless otherwise specified (I, cross-nicols).

In contrast, the thicker organic-poor laminae are composed of anhedral carbonate crystals ranging from a few microns to nearly 50 μm in diameter. Fine-grained micrite appears cloudy under plane-polarized light, whereas coarser crystalline layers are noticeably clearer. These laminae contain little to no detrital quartz but preserve faint, 0.3–0.5 mm "ghosts" of rounded grains, including one particularly prominent cloudy grain (Fig. 5). Several unidentified microfossils, including chambered multilocular tests and calcified circular structures, are also preserved within the micrite (Fig. 6).

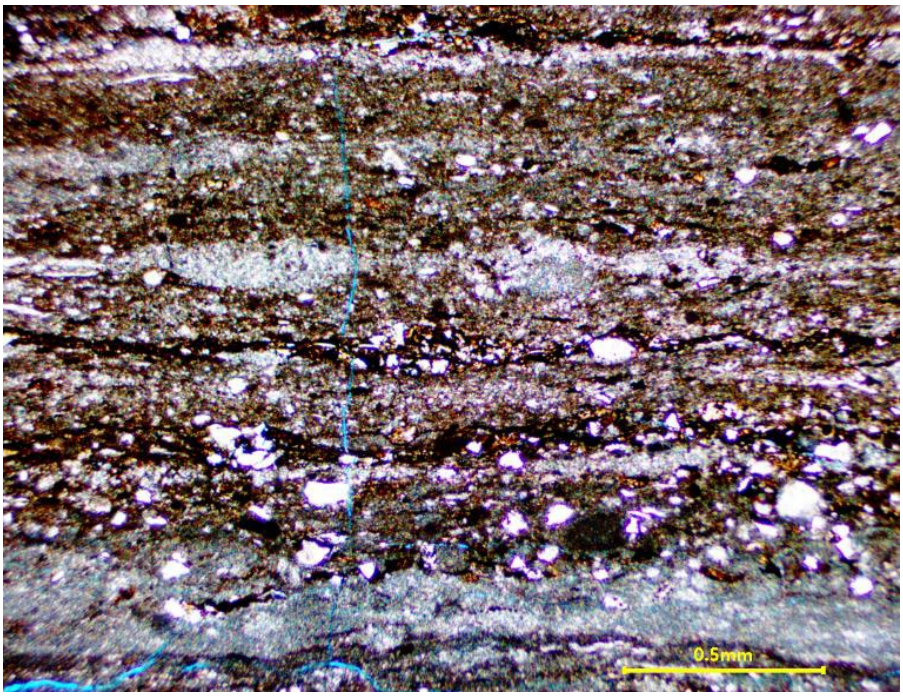

Figure 3. Plane-polarized light photomicrograph of organic-rich lamina at 7,379.90 ft. Fabric contains wavy organic strands (black), dispersed silt-sized quartz grains (bright white), and discontinuous, lensoidal micro-laminae of clear micrite embedded in a dark matrix. Scale bar is 0.5 mm.

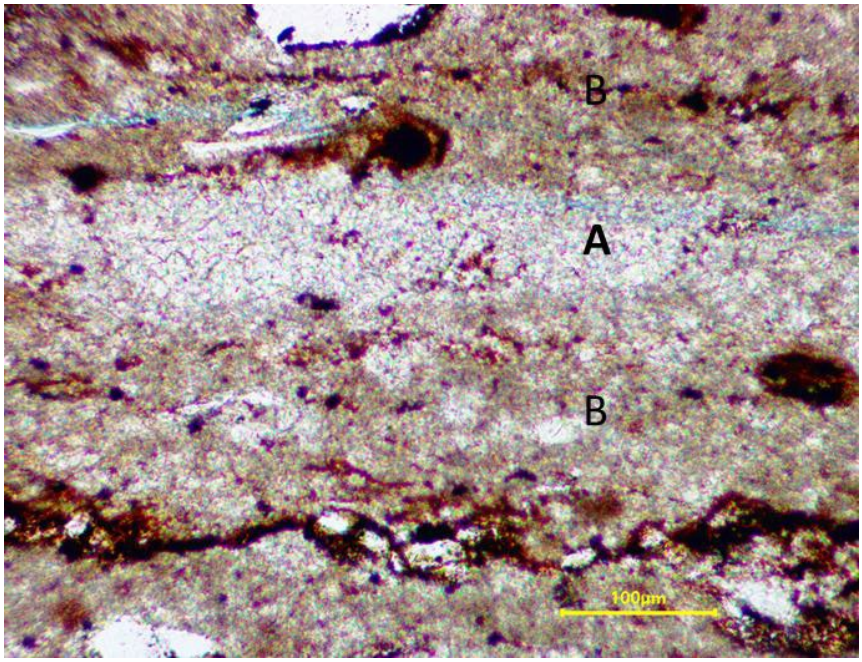

Figure 4. High-magnification photomicrograph (plane light) at 7,379.90 ft showing a discontinuous, clear micrite micro-lamina (A) nested within dark, organic-rich micrite laminae (B). Scale bar is 100 µm.

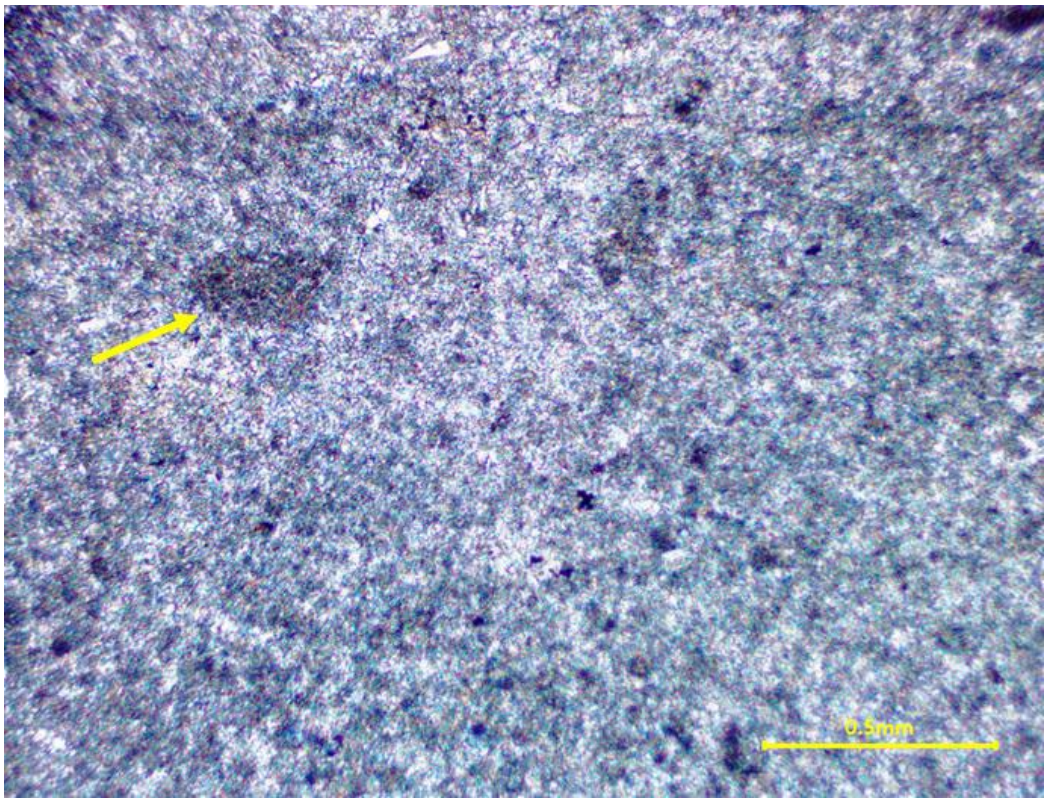

Figure 5. Plane light photomicrograph of organic-poor laminae showing faint "ghosts" of rounded grains (0.3–0.5 mm). Yellow arrow denotes a prominent cloudy grain. Note the conspicuous absence of detrital quartz relative to Figure 2. Scale bar is 0.5 mm.

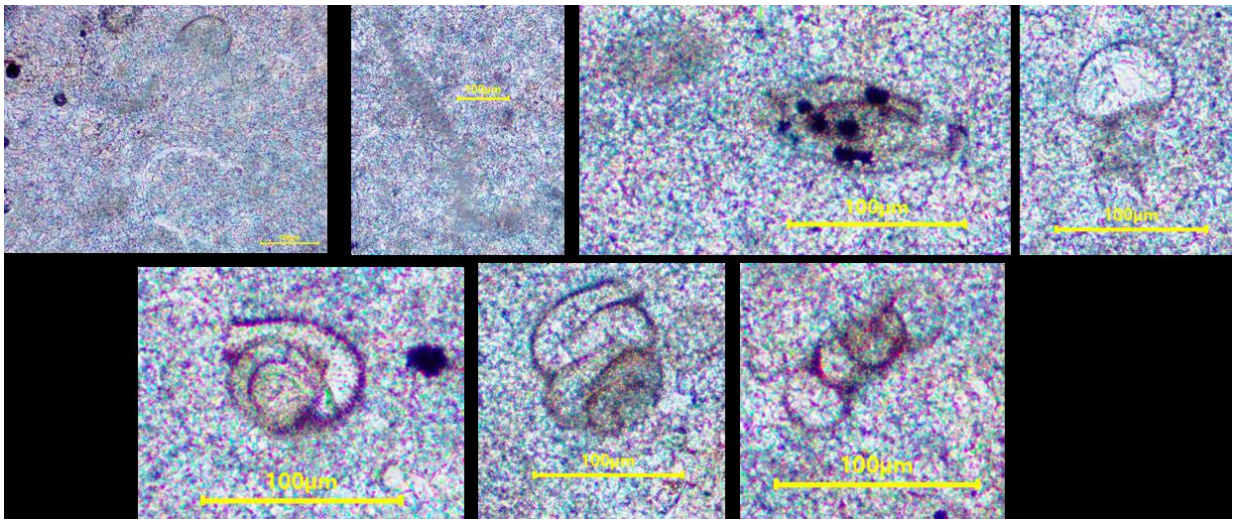

Figure 6. Composite photomicrographs (plane light) at 7,379.90 ft showing unidentified microfossils within the micrite matrix, including multi-locular chambered tests and ovate bioclasts. Scale bars are 100 µm.

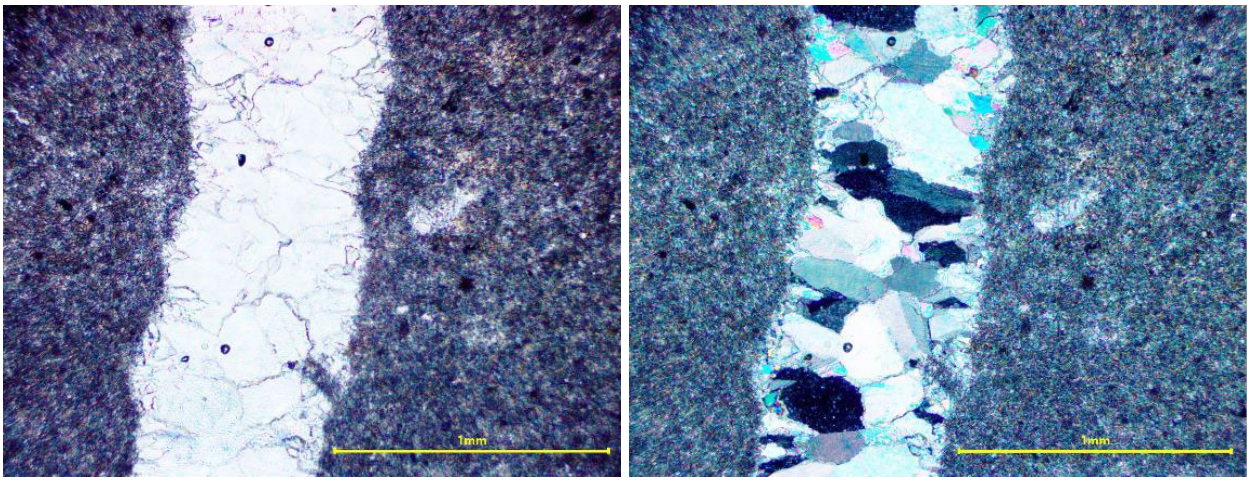

Figure 7. Photomicrographs of a clear carbonate-filled microfracture within organic-poor micrite under plane light (left) and cross-polarized light (right). The fracture terminates at the organic-rich laminae boundaries and displays a drusy fabric with crystal sizes increasing toward the center. Scale bar is 1 mm.

Late-stage, carbonate-filled microfractures crosscut the organic-poor laminae but terminate against—or locally originate at—the adjacent organic-rich laminae without penetrating them. Under crossed polars, these fractures display a drusy cement fabric, with crystal size increasing toward the center (Fig. 7).

Interpretation:

The alternating organic-rich and organic-poor micritic laminae indicate deposition in a low-energy marine environment, probably below storm wave base, where fine carbonate mud accumulated with little physical disturbance. The preservation of delicate micro-lamination, together with the absence of bioturbation and the occurrence of micron-scale framboidal pyrite, indicates persistently oxygen-deficient bottom waters ranging from dysoxic to anoxic. The randomly dispersed silt-sized quartz grains and mica flakes within the organic-rich laminae are interpreted to represent eolian detritus rather than traction-transported sediment. Their enrichment in the organic-rich intervals, alongside higher organic matter concentrations, suggests periods of reduced carbonate sedimentation that concentrated both siliciclastic detritus and organic material relative to the cleaner carbonate laminae.

7,418.05 feet Interval (Peloidal Packstone)

The sample at 7,418.05 ft consists of a coarse-grained, poorly sorted peloidal packstone that contrasts sharply with the fine-grained laminated mudstones above and below. The rock contains a heterogeneous mixture of peloids up to 1.5 mm in diameter, abundant *Favreina* fecal pellets, and skeletal bryozoan fragments (Figs. 8, 9). The *Favreina* pellets are readily recognized by their characteristic parallel longitudinal tubes (Fig. 9). Isolated, irregular voids of uncertain origin are filled by coarse, blocky calcite cement, whereas localized primary intraparticle porosity is preserved within bryozoan molds (Fig. 8, lower left).

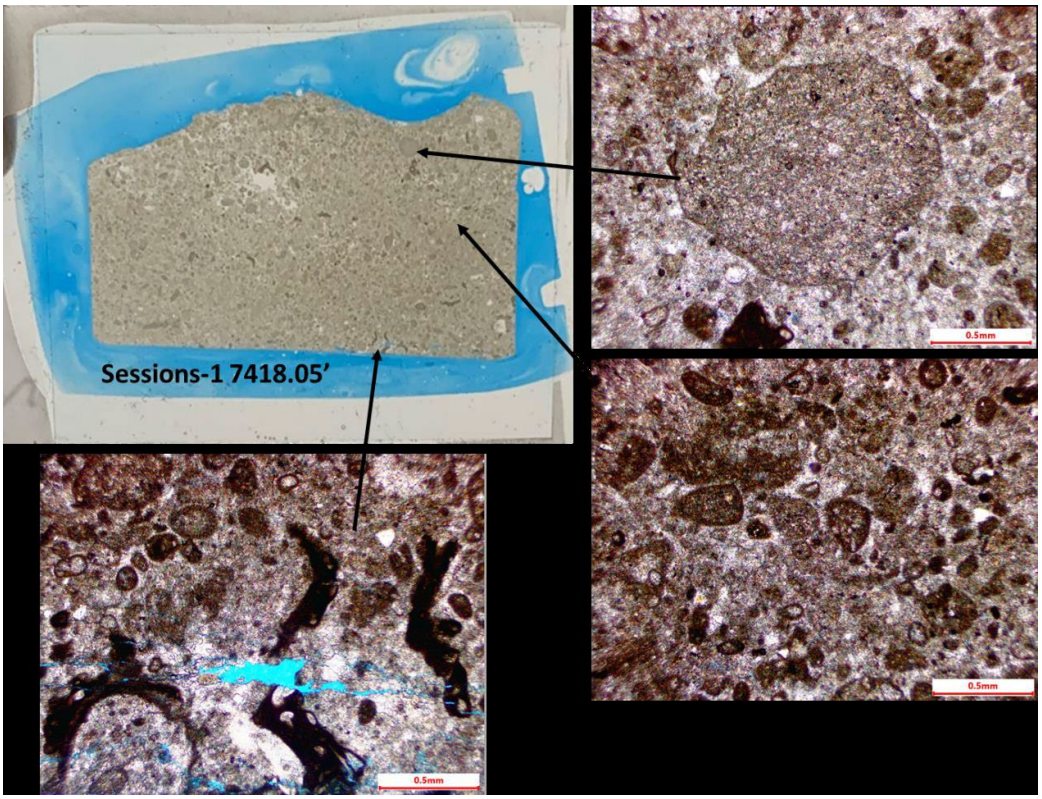

Figure 8. Thin section overview and photomicrographs of a poorly sorted peloidal packstone at 7,418.05 ft. Upper right: close-up of a large peloid. Lower right: representative grain size and poor sorting of the peloidal matrix. Lower left: bryozoan skeletal fragments and associated porosity (blue epoxy). All scale bars are 0.5 mm.

Interpretation:

The coarse grain size, grain-supported texture, and abundance of skeletal bioclasts and *Favreina* fecal pellets indicate deposition under substantially higher-energy conditions than those represented by the laminated mudstones. Although the poor sorting suggests fluctuating flow conditions rather than prolonged wave reworking, the assemblage is consistent with a shallow, open-marine environment. This packstone represents a pronounced lithofacies contrast with the fine-grained, organic-rich mudstones located only 38.15 ft above and 23.85 ft below, indicating that it records a relatively brief departure from the prevailing depositional conditions.

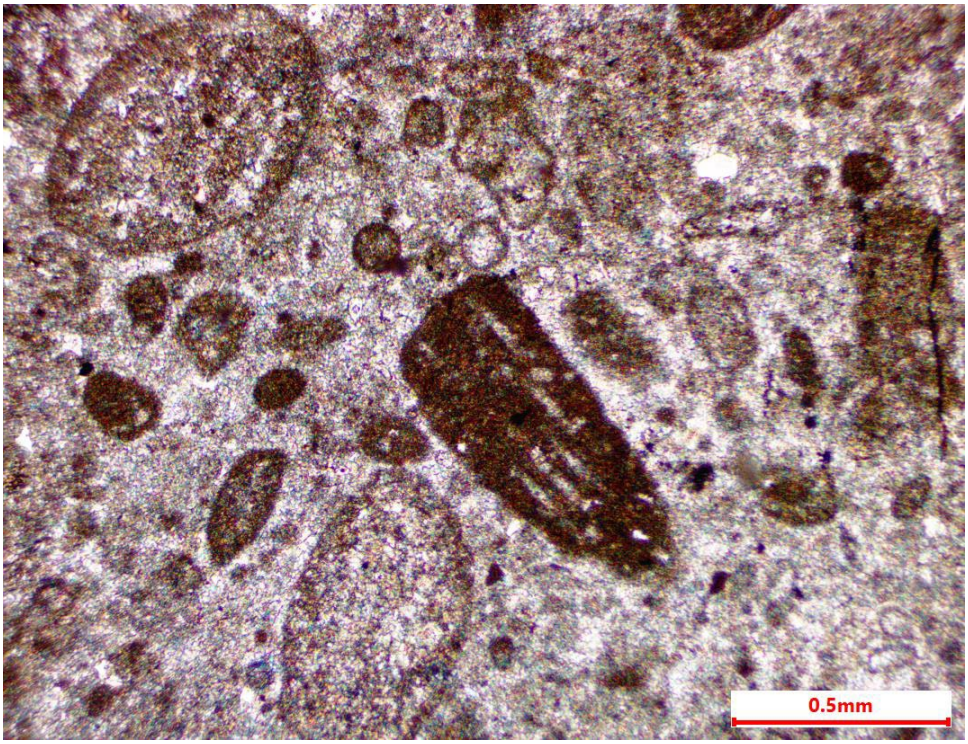

Figure 9. Photomicrograph (plane light) at 7,418.05 ft displaying a distinctive *Favreina* fecal pellet (center) characterized by internal, parallel longitudinal tubes. The pellet is surrounded by a poorly sorted peloidal packstone matrix. Scale bar is 0.5 mm.

Two depositional models can explain the observed fabric. The interval is interpreted to represent a short-lived shoaling event from a high-frequency relative sea-level fall that temporarily shifted deposition above storm wave base. Alternatively, it could record the redeposition of shallow-water skeletal and peloidal sediment into deeper water by a sediment-gravity flow, such

as a debris flow or turbidite. The available petrographic observations do not uniquely distinguish between these two interpretations.

7,441.90 feet Interval (Dolomitic Siltstone/Micritic Mudstone)

The sample at 7,441.90 ft consists of two contrasting microfacies: a basal organic-rich dolomitic siltstone overlain by finely interlaminated micritic mudstones (Fig. 10). This interval differs markedly from the two overlying samples by containing abundant siliciclastic material and clay minerals alongside carbonate. This unique composition makes it particularly suitable for evaluating lithium partitioning between organic and inorganic components.

The basal portion of the thin section comprises a dense, organic-rich dolomitic siltstone of tightly packed, silt-sized rhombohedral carbonate crystals interpreted as dolomite (Fig. 10, lower panels). Dark intergranular organic matter is abundant throughout this facies. Elongate lenses of clear micrite, typically less than 0.1 mm thick and up to 1 mm long, occur as sharply bounded layers within the dolomitic fabric and commonly contain dispersed organic inclusions (Fig. 10, lower right). Dispersed silt- to very fine sand-sized quartz grains make up an estimated 5% or less of the rock.

The upper portion of the thin section grades into finely interlaminated micrite and organic-rich siltstone (Fig. 10, upper panels). Discontinuous organic-rich micro-laminae are associated with dispersed silt-sized quartz grains and trace amounts of white mica (muscovite/illite). The close juxtaposition of organic-rich and organic-poor laminae within this interval permitted selective micro-sampling of the contrasting fabrics for subsequent lithium isotope and TOC analyses.

Late-stage diagenetic features include carbonate-filled microfractures that crosscut the primary depositional fabric and coarse, tabular barite crystals localized along these fractures. A highly reflective slickenside or shear surface observed in the hand specimen is interpreted to correspond to one of these barite-mineralized fracture planes.

Bulk-rock X-ray diffraction data from Li et al. (2016) indicate that this interval contains approximately 19 wt.% clay, consisting of mixed-layer illite/smectite and discrete illite (Table 1). The elevated clay content, alongside abundant detrital quartz and closely paired organic-rich and

organic-poor microfacies, distinguishes this interval from overlying carbonate-dominated samples and drove its selection for lithium isotope investigation.

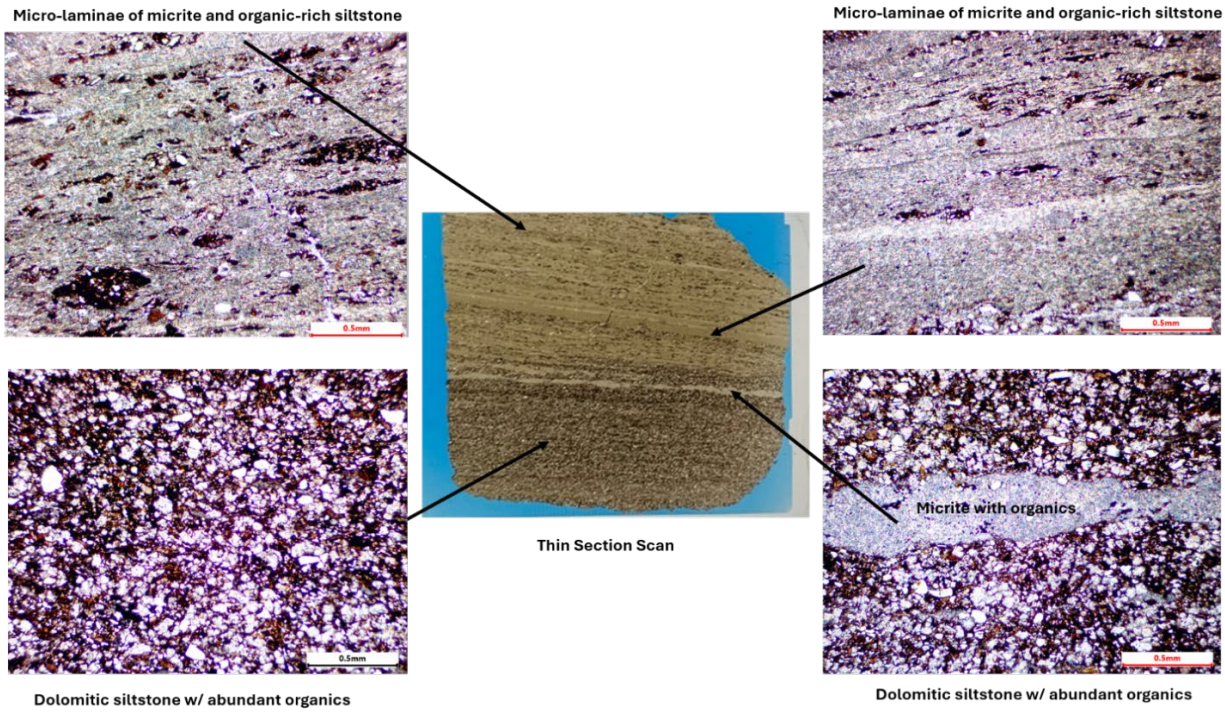

Figure 10. Thin section scan and plane-light photomicrographs at 7,441.90 ft. Lower panels: coarse, rhombohedral dolomitic siltstone with abundant organic matter (left) and a distinct, sharp-walled micrite layer with organic inclusions (right). Upper panels: finely interlaminated micrite and organic-rich siltstone highlighting low-angle downlapping geometries. All scale bars are 0.5 mm.

Interpretation:

Similar to the 7,379.90-ft interval, the fine-grained sediment, abundant organic matter, and preservation of delicate micro-lamination indicate deposition below storm wave base in a low-energy marine setting. However, low-angle downlapping micro-clinoforms demonstrates that intermittent, traction-driven bottom currents influenced deposition. The transition from continuous lamination into discontinuous concentrations of organic matter within these downlapping packages suggests that fluctuating current velocities locally disrupted and redistributed previously continuous organic-rich laminae during or shortly after deposition. Despite this episodic hydrodynamic reworking, the widespread preservation of delicate lamination and abundant labile

organic matter indicates that sediment disturbance remained limited and that bottom waters persisted under dysoxic to anoxic conditions.

Table 1. Whole rock X-ray diffraction (XRD) mineralogical data for the Lower member of the Smackover Formation core sample intervals (modified from Li et al., 2016). Values are reported in weight percent.

Sample	Sample	CLAYS				CARBONATES			OTHER MINERALS					TOTALS		
Number	Depth (ft)	Chlorite	Kaolinite	Illite/Mica	Mx I/S*	Calcite	Dolomite[1]	Siderite	Quartz	K-spar	Plag.	Pyrite	Barite	Clays	Carb.	Other
1-5RMV	7379.90	Tr	Tr	1	Tr	97	Tr	Tr	2	Tr	Tr	Tr	0	1	97	2
1-44RMV	7418.05	Tr	Tr	1	Tr	97	Tr	Tr	2	Tr	Tr	Tr	0	1	97	2
2-7RMV	7441.90	Tr	2	13	4	31	18	Tr	26	Tr	3	3	0	19	49	32
	Average	Tr	1	5	1	75	6	Tr	10	Tr	1	1	0	7	81	12

Tr = Trace.
* Ordered interstratified mixed-layer illite/smectite; Approximately 10-20% expandable interlayers.
[1] Dolomite species interpretation based on the d-spacing of the highest intensity peak of dolomite group minerals; other dolomite species may be present.

LITHIUM ISOTOPIC ANALYSIS

Sample Selection and Analytical Methods

The sample interval from 7,441.90 ft was selected for coupled TOC and lithium isotope analysis. This depth was chosen because its significantly elevated clay (19%) and detrital quartz (26%) content provided the necessary silicate-rich matrix to evaluate lithium behavior relative to the pure carbonate intervals found elsewhere in the core (Table 1). To assess micro-spatial geochemical variability between co-existing microfacies, the dark, organic-rich (lower portion of the thin section) and lighter, organic-poor laminae (upper portion of the thin section) were micro-subsampled.

Bulk analytical results demonstrate a strong geochemical partitioning between the two fabrics (Table 2). The measured lithium isotopic composition (δ^7Li) of the organic-rich matrix (+1.1‰) is significantly lighter (more depleted in δ^7Li) than that of its organic-poor counterpart (+9.0‰). This isotopic depletion correlates with an increase in TOC content from 0.11 wt.% in the organic-poor laminae to 2.76 wt.% in the organic-rich laminae, as well as an elemental lithium enrichment from 2.8 ppm to 3.9 ppm, respectively (Table 2).

Table 2. Geochemical data and lithium isotope compositions of core subsamples at 7,441.90 ft.

Subsample Type	δ^7Li ‰ (LSVEC)	2 Standard Deviations*	Li Concentration (ppm)	Leco TOC (wt%)	Inorganic Fraction (wt%)
Organic-poor laminae	+9.0	0.5	2.8	0.11	99.89
Organic-rich laminae	+1.1	0.5	3.9	2.76	97.24

*Uncertainties based on repeated measurements of IAPSO seawater (n = 22).

Two-Component Mass-Balance Modeling

To isolate the true isotopic signature of the organic phase, the differential microfacies values were utilized to construct a two-component linear mass-balance model. The total measured elemental lithium concentration is defined by the relative weight fractions (f) of the organic and inorganic components:

$$[\mathrm{Li}]_{\mathrm{meas}} = (f_{\mathrm{org}} \times [\mathrm{Li}]_{\mathrm{org}}) + (f_{\mathrm{inorg}} \times [\mathrm{Li}]_{\mathrm{inorg}})$$

Substituting the empirical weight fractions (derived from the Leco TOC values in Table 2) generates a system of two linear equations for the individual laminae pools:

$$\text{Organic-poor laminae: } 2.8 \text{ ppm} = (0.0011 \times [\mathrm{Li}]_{\mathrm{org}}) + (0.9989 \times [\mathrm{Li}]_{\mathrm{inorg}})$$

$$\text{Organic-rich laminae: } 3.9 \text{ ppm} = (0.0276 \times [\mathrm{Li}]_{\mathrm{org}}) + (0.9724 \times [\mathrm{Li}]_{\mathrm{inorg}})$$

Simultaneous solution of this system yields an isolated lithium concentration of 44.3 ppm within the pure organic end-member phase and 2.75 ppm within the pure inorganic matrix (Table 3).

Using these isolated elemental concentrations, the isotopic composition (δ^7Li) of each discrete phase can be mathematically resolved by weighting the isotopic signatures against their respective elemental mass fractions:

$$\delta^7\mathrm{Li}_{\mathrm{meas}} = \frac{\left(f_{\mathrm{org}} \times [\mathrm{Li}]_{\mathrm{org}} \times \delta^7\mathrm{Li}_{\mathrm{org}}\right) + \left(f_{\mathrm{inorg}} \times [\mathrm{Li}]_{\mathrm{inorg}} \times \delta^7\mathrm{Li}_{\mathrm{inorg}}\right)}{[\mathrm{Li}]_{\mathrm{meas}}}$$

Substituting the measured isotopic values and calculated concentrations defines the isotopic balance for each micro-subsample:

$$\text{Organic} - \text{poor laminae: } +9.0 = \frac{\left(0.0011 \times 44.3 \times \delta^{7}\text{Li}_{\text{org}}\right) + \left(0.9989 \times 2.75 \times \delta^{7}\text{Li}_{\text{inorg}}\right)}{2.8}$$

$$\text{Organic} - \text{rich laminae: } +1.1 = \frac{\left(0.0276 \times 44.3 \times \delta^{7}\text{Li}_{\text{org}}\right) + \left(0.9724 \times 2.75 \times \delta^{7}\text{Li}_{\text{inorg}}\right)}{3.9}$$

Solving this second system of equations isolates a calculated $\delta^{7}\text{Li}_{\text{org}}$ of -17.2‰ for the pure organic phase and a $\delta^{7}\text{Li}_{\text{inorg}}$ of +9.5‰ for the inorganic matrix end-member (Table 3).

Global Context and Geochemical Interpretation

The organic-rich and organic-poor laminae exhibit a pronounced isotopic contrast ($\delta^{7}\text{Li}_{\text{op-or}}$ = 7.9‰) accompanied by distinct differences in lithium concentration and TOC content. The relatively heavy isotopic composition (+9.0‰) and very low TOC (0.11 wt.%) of the organic-poor laminae closely match the calculated inorganic end-member (+9.5‰). This close agreement indicates that the measured lithium isotope composition is dominated by the inorganic mineral fraction.

In contrast, the two-component mass-balance model yields a calculated organic end-member containing 44.3 ppm lithium with a δ^{7}Li value of -17.2‰. Under the assumptions of the model, this large isotopic difference indicates that lithium in the organic fraction is strongly enriched in the lighter isotope (^{6}Li) relative to the coexisting inorganic matrix. Although the exact fractionation mechanism cannot be determined from these data alone, the results are consistent with preferential incorporation of ^{6}Li into organic matter during deposition and/or early diagenesis through biological, chemical, or kinetic processes.

To place these results in a broader context, Teichert et al. (2020) compiled lithium isotope compositions from a wide range of U.S. coals and petroleum source rocks. Most organic-rich materials exhibit distinctly negative δ^{7}Li values, with petroleum source rocks generally having somewhat heavier compositions than coals (Fig. 11). Under the assumptions of the present mass-balance model, the calculated Lower Smackover organic end-member (-17.2‰) falls well within this published range, sitting near the upper, less negative end of the petroleum source-rock population (Fig. 11, yellow star). This agreement provides independent support for the model's

plausibility and suggests that the inferred isotopic composition is representative of lithium associated with sedimentary organic matter.

Table 3. Calculated lithium concentrations and isotopic compositions (δ^7Li) for organic and inorganic phases within the 7,441.90 ft sample interval.

Phase	Li Concentration (ppm)	Isotopic Composition (δ^7Li ‰)
Organic	44.3	-17.2
Inorganic	2.75	+9.5

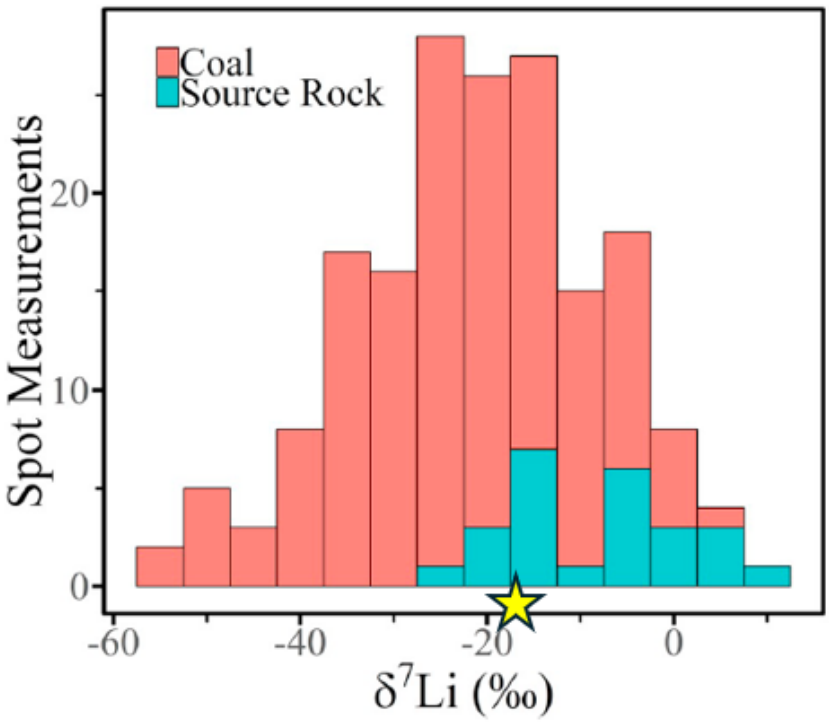

Figure 11. Comparison of the calculated Lower member of the Smackover organic matter δ^7Li composition (yellow star) against a global compilation of organic lithium isotope signatures from coals and petroleum source rocks (modified from Teichert et al., 2020).

CONCLUSIONS

This study integrates petrographic observations, TOC analyses, lithium concentrations, and lithium isotope measurements to characterize lithium partitioning within the Lower member of the Smackover Formation. The principal conclusions are:

1. Petrographic examination identified three distinct lithofacies across three samples, with the 7,441.90-ft interval containing closely paired organic-rich and organic-poor microfacies ideal for comparative geochemical analysis.

2. A two-component mass-balance model indicates that the organic fraction contains substantially higher lithium concentrations (44.3 ppm) than the inorganic matrix (2.75 ppm).

3. Under the assumptions of the mass-balance model, the calculated organic end-member has a δ^7Li value of −17.2‰, whereas the inorganic fraction yields a value of +9.5‰.

4. The inferred organic δ^7Li value falls within the range reported for petroleum source rocks by Teichert et al. (2020), supporting the interpretation that lithium associated with organic matter is isotopically distinct from the surrounding inorganic matrix.

5. These results demonstrate that combining petrography with lithium isotope geochemistry provides a practical approach for estimating the isotopic composition of organic matter in sedimentary rocks when direct separation of pure organic material is unfeasible.

REFERENCES

Li, P., M.E. Ratchford, M.W. Charette, B.J. Walls, and R.P. Philip, 2016, Unconventional reservoir characterization of the Brown Dense Mudstone (Lower Smackover Formation), Gulf Coastal Plain, South Arkansas, Gulf Coast Association of Geological Societies Transactions, v. 66, p. 335-352.

Teichert, Z., M. Bose, and L.B. Williams, 2020, Lithium isotope composition of U.S. coals and source rocks: potential tracer of hydrocarbons, Chemical Geology, v. 549, art. 119694, https://doi.org/10.1016/j.chemgeo.2020.119694.